arXiv:cond-mat/0101217v1 [cond-mat.supr-con] 15 Jan 2001

Superconductivity-induced changes of the phonon resonances in $R\mathrm{Ba_2Cu_3O_7}$ (R = rare earth)

S. Ostertun, J. Kiltz, A. Bock*, and U. Merkt
Institut für Angewandte Physik und Zentrum für Mikrostrukturforschung, Universität Hamburg, Jungiusstraße 11, D-20355 Hamburg, Germany

T. Wolf
Institut für Festkörperphysik, Forschungszentrum Karlsruhe, D-76021 Karlsruhe, Germany

(February 1, 2008)

We observe a characteristic energy $\hbar\omega_c \approx 2.1$ eV which separates regions of different behavior of the phonon intensities in the Raman spectra of the $R\mathrm{Ba_2Cu_3O_7}$ system. A superconductivity-induced drop of phonon intensities is found for the oxygen modes O(4) and O(2)-O(3) only for excitation energies below $\hbar\omega_c$. This intensity drop indicates an order parameter which affects energies in the vicinity of $\hbar\omega_c$.

PACS numbers: 74.25.Gz, 74.25.Jb, 74.25.Kc, 74.72.Bk, 78.30.Er

I. INTRODUCTION

Several superconductivity-induced changes of parameters describing the phonons in the cuprate superconductors can be determined by Raman spectroscopy. Frequency and linewidth anomalies like hardening and broadening have been the subject of several experimental[1–3] and theoretical[4–7] studies. While the superconductivity-induced phonon self-energy effects allow conclusions regarding the order parameter only for energies similar to the phonon energies (up to 100 meV), high-energy (>1 eV) questions cannot be addressed this way. Resonant Raman scattering is an experimental technique which allows one to examine the physics at high energy through the resonances of phonons. In contrast to reflectivity or transmission spectroscopy the affected phonons provide direct information on incorporated electronic bands as the assignments of the phonon modes in the spectra to the vibrating atoms is well known through group theoretical calculations and isotope substitution experiments. Thus, the dependence of the phonon intensities on temperature and excitation energy can provide information about the scattering mechanism and especially about the superconducting state.

In contrast to the usually observed increase of the intensity[8,9] below the critical temperature T_c we observe a drop of intensity in several modes when exciting with photons of energy $\hbar\omega_i < 2.1$ eV. In the same region of excitation energy the apical oxygen mode at 500 cm^{-1} shows a violation of the symmetry selection rule which cannot be explained in terms of an orthorhombic distortion. Summarizing our data we conclude that the origin of the intensity anomaly is related to a modification of the Cu-O charge transfer mechanism in the superconducting state in comparison to the normal state.

II. EXPERIMENTAL DETAILS

Subject of this paper are Yb-123, Er-123, Sm-123 and Nd-123 single crystals, with T_c = 76 K, 81 K, 94 K, and 90 K, respectively. All measured single crystals were grown with a self-flux method and annealed with oxygen under high pressure.[10] Due to the high oxygen content and the different radii of the rare earth atoms Yb-123 and Er-123 are overdoped whereas Sm-123 and Nd-123 are nearly optimally doped.[11] The laser beam is focused onto the sample along the c-direction. The orthorhombic symmetry of the R-123 system can be treated as tetragonal. Accordingly, the Raman active phonons are of $\mathrm{A_{1g}}$ and $\mathrm{B_{1g}}$ symmetry, which are allowed for $\mathrm{z(xx)\bar{z}/z(x'x')\bar{z}}$ and $\mathrm{z(xx)\bar{z}/z(x'y')\bar{z}}$ polarizations in the Porto notation, respectively. All polarizations are specified with respect to the axes along the Cu-O bonds of the $\mathrm{CuO_2}$ planes, primed polarizations are rotated by 45°. For simplicity z and $\bar{\mathrm{z}}$ are omitted in the following. The measurements were performed using several lines of $\mathrm{Ar^+}$, He-Ne and Ti:Saphir lasers in quasi-backscattering geometry. The details of the setup are described elsewhere.[12] In order to achieve a high accuracy of intensity measurements the laser power was monitored during the measurements. All spectra were corrected for the response of the detector and the optical system. Also, they are normalized to the incident photon rate.

For a comparison of intensities obtained with different excitation energies the cross-section is calculated from the efficiencies using ellipsometric data of Yb-123. The complex dielectric function of Bi-2212 shows only a slight variation with temperature[13] at our excitation energies between 1.68 eV and 2.71 eV and the resulting reflectivity exhibits maximal variations below 1%. As the reflectivity of the R-123 system behaves similar,[14] Raman spectra of all temperatures can be evaluated with the ellipsometric data obtained at room-temperature. In Fig. 1 the complex dielectric function of Yb-123 at room-temperature is given. From the real part ε_1 of the dielectric function we can estimate a screened plasma frequency ω_p of 1.44 eV.

The low-temperature background intensity of the cross-section at $\omega \approx 700$ cm^{-1} is plotted versus the excitation energy for the x'x' and x'y' polarization geometry in the inset of Fig. 1 in the top and bottom panel, respectively. Within experimental error no significant resonance of the cross-section can be determined. The scattering of the data points results from uncertainties in the adjustment of the setup. Thus, the measured phonon intensities will scatter in a similar way. To obtain the integrated phonon intensities we fitted the spectra to the model presented in a previous paper.[3] An extended Fano profile is described by

$$I(\omega) = \frac{C}{\gamma(\omega)\left[1+\epsilon^2(\omega)\right]} \times \left\{ \frac{R_*^2(\omega)}{C^2} - 2\epsilon(\omega)\frac{R_*(\omega)\varrho_*(\omega)}{C^2} - \frac{\varrho_*^2(\omega)}{C^2} \right\} \qquad (1)$$

with the substitutions $\varrho_*(\omega) = C g_\sigma^2 \varrho_\sigma^e(\omega)$, $R_*(\omega) = C g_\sigma^2 R_\sigma^e(\omega) + R_0$, $\epsilon(\omega) = \left[\omega^2 - \omega_\nu^2(\omega)\right]/2\omega_p\gamma(\omega)$, $\gamma(\omega) = \Gamma + \varrho_*(\omega)/C$, and $\omega_\nu^2(\omega) = \omega_p^2 - 2\omega_p R_*(\omega)/C$. Here, $\varrho_\sigma^e(\omega)$ and $R_\sigma^e(\omega)$ are the imaginary and real part of the electronic response function, respectively, and g_σ is the lowest-order expansion coefficient of the electron-phonon vertex. The bare frequency and linewidth of the phonon are ω_p and Γ, respectively. The constant C is a scaling parameter due to the use of arbitrary units in the spectra.

We use this extended Fano profile for the asymmetric phonon modes and Lorentzian profiles for the remaining phonons. As described in Ref. 3, the measured electronic response $\varrho_*(\omega)$ is described via a phenomenological formula which contains a $\tanh(\omega/\omega_T)$ term for the incoherent background and two coupled Lorentzian profiles for the redistribution of the spectra below T_c — one for the pair breaking peak and a negative one for the suppression of spectral weight at low Raman shifts. This formula allows a simultaneous description of $R_*(\omega)$.

III. RESULTS

In the top panels of Fig. 2 we present spectra of Yb-123 obtained at 15 K nominal temperature in x'x' ($\mathrm{A_{1g}}+\mathrm{B_{2g}}$) and in x'y' ($\mathrm{B_{1g}}$) geometry with excitation energies of 2.71 eV and 1.96 eV. The original spectra have been scaled to equal background intensity for clarity. Exciting with 2.71 eV all phonons show up mainly in the spectra of the expected polarization geometry. For the x'x' geometry we have the Ba mode at 120 cm^{-1}, Cu(2) at 150 cm^{-1}, O(2)+O(3) at 440 cm^{-1}, and O(4) at 500 cm^{-1}. For the x'y' geometry the O(2)-O(3) mode appears at 340 cm^{-1}. In contrast, exciting with 1.96 eV the O(4) mode has nearly vanished in x'x' geometry but only slightly changed in x'y' symmetry. Nearly the same behavior is observed for the resonance of the intensity of the O(4) mode in Er-123, Sm-123, and Nd-123. Orthorhombic distortion, which is usually mentioned as the cause for phonon intensity in forbidden symmetries, cannot explain this behavior. Though resonance effects can disturb symmetry selection rules in principle, the symmetry violation should appear under resonance conditions but not out of resonance.

Subtracting the phononic contribution we get the electronic background of Yb-123, which is plotted in the lower panels of Fig. 2. The x'x' spectra are nearly identical for both excitation energies and even the x'y' spectra are quite similar. The $\mathrm{B_{1g}}$ pair breaking peak lies at a relatively low energy of 320 cm^{-1} due to the high doping level[15] of $p \approx 0.2$, which is determined from $T_c/T_{c,\mathrm{max}}$ (see Ref. 16). There is no enhancement of the gap excitation from 1.96 eV to 2.71 eV. This is consistent with the behavior observed for Bi-2212 which shows non-resonant gap excitations for doping levels up to approximately 0.2 and a gap resonance only for higher doping levels as reported in Ref. 17.

Figure 3 depicts the results of a detailed study of the integrated O(4) mode intensity. For temperatures above T_c the x'x' intensity increases when the temperature is lowered for excitation energies of 1.96 eV, 2.41 eV, and 2.71 eV. This increase is hardly influenced by the phase transition below T_c for 2.41 eV and 2.71 eV in contrast to 1.96 eV where the intensity suddenly drops. The comparatively high values for intensities of the 2.71 eV data in the range of 100 K to 200 K are due to the scattering mentioned in the introduction. Here it results from a slight shift of the laser spot with respect to the entrance slit of the spectrometer. On the other hand the x'y' intensity shows the same behavior for all measured excitation energies: a slight increase with decreasing temperature not or only slightly affected by T_c. For temperatures above T_c the relation for the x'x' intensities $I_{2.71}$:$I_{2.41}$:$I_{1.96}$ is approximately 5.0:3.1:1.0 as indicated by the solid lines in the left panel of Fig. 3. The superconductivity-induced drop of the x'x' intensity at low excitation energies leads to a superconductivity-induced enhancement of the resonance profile of the x'x' O(4) mode intensity.

Figure 4 yields the excitation energy $\hbar\omega_c = 2.1 \pm 0.1$ cm^{-1} where the O(4) mode exhibits equal intensity in x'x' and x'y' geometries. This is also the energy of the crossover between the superconductivity-induced increase and decrease of the x'x' intensity shown in Fig. 3, i. e. 2.0-2.4 eV. While the measurements have been carried out in this detail for Yb-123 only, spectra of Er-123, Sm-123, and Nd-123 at low temperature exhibit a similar behavior as shown in the inset of Fig. 4. There the ratio of the x'x' and x'y' O(4) mode intensity is plotted against the excitation energy. It exhibits no significant doping dependence. The O(2)-O(3) mode displays a similar behavior in the x'y' as the O(4) mode in the x'x' symmetry. In Fig. 5 the temperature dependence of its intensity is plotted for excitation energies $\hbar\omega_i = 1.68$ eV, 1.96 eV, 2.41 eV, and 2.71 eV. Above T_c the intensity is only slightly affected by the temperature, below T_c the intensity drops only for excitation energies below $\hbar\omega_c$.

The intensity of the Cu(2) mode shows a strong increase with decreasing temperature above T_c but also a slight drop below T_c. The intensity at low temperatures is approximately 70%–80% of the highest value at T_c. While this ratio is independent of excitation energy and polarization geometry the resonance energy itself depends on the polarization geometry as shown in Fig. 6. Gaussian profiles guide the eye and help to determine the resonance energy of the Cu(2) mode intensity, which is about 2.1 eV for x'x' and well below 2.0 eV for x'y' symmetry. The Ba mode which is not shown here exhibits a slight intensity gain below T_c, which seems to be unaffected by $\hbar\omega_c$. The x'x' intensity is resonant at 2.6 eV or even higher energy, the x'y' intensity follows this profile with about 30% of the intensity in x'x' geometry.

IV. DISCUSSION AND CONCLUSIONS

Summarizing our data we find a characteristic energy $\hbar\omega_c \approx 2.1$ eV which separates the regions of red and blue excitations. It is very similar to the crossing point at 2.2 eV observed in the imaginary part of the dielectric function[13] of Bi-2212. For red excitation the *R*-123 system exhibits a superconductivity-induced drop of the intensity of the O(4) mode in x'x' and the O(2)-O(3) mode in x'y' symmetry, for blue excitation the drop is absent. Additionally, for red excitations the symmetry selection rule of the O(4) mode is violated as the x'y' intensity exceeds the x'x' intensity. The maximum of the intensity of the Cu(2) mode in x'x' symmetry coincides with $\hbar\omega_c$. All these effects are characterized by $\hbar\omega_c$ indicating a common microscopic origin. Low temperature measurements of overdoped Er-123 as well as of underdoped Sm-123 and Nd-123 show a similar behavior as Yb-123, especially the symmetry violation of the O(4) mode for excitation energies below $\hbar\omega_c$. Thus $\hbar\omega_c$ could be a general property of the *R*-123 system without a significant doping dependence.

Friedl *et al.*[18] observed a superconductivity-induced gain of the xx phonon intensities of Y-123 films on $SrTiO_3$ substrates, which are independent of excitation energy in the range of 1.92 eV to 2.60 eV, a drop of intensity is observed only for the Cu(2) mode. The differences between their data and the data presented here may in principle result from the different doping levels of Y-123 and Yb-123. But as we have noted above, the effects are mainly independent of doping, our explanation for the discrepancies between Friedl's and our data is the following: As the lattice constant of Y-123 (3.82/3.88 Å) is smaller than that of $SrTiO_3$ (3.91 Å) and as the thermal expansion coefficient of Y-123 (11.7 Å/K) exceeds that of $SrTiO_3$ (9.4 Å/K), the lattice mismatch increases with decreasing temperature. The additional stress may explain the high intensity increase I(100K):I(250K)≈2.5 of the Y-123 films in comparison to I(100K):I(300K)≈1.3 of the Yb-123 single crystal. Thus, the drop below T_c is masked in this strong increase, especially as Friedl *et al.* recorded xx+yy data which include x'y' where no intensity drop appears. In underdoped *R*-123 the O(2)-O(3) mode is known to show a strong intensity gain.[3] Thus, the intensity drop of the O(2)-O(3) mode can only be observed in overdoped samples as the drop is not masked by an intensity gain.

Sherman *et al.*[8] explained the increase of the total B_{1g} mode intensity below T_c of Y-123 in terms of an extension of the number of intermediate electronic states near the Fermi surface that participate in the Raman process. Accordingly, the doping dependence of the gain of the O(2)-O(3) mode intensity can be explained in this picture by the vicinity to the Fermi-level. Analogously, an intensity drop means a reduction of the number of intermediate states which is not consistent with this model. Possibly the intensity gain and the intensity drop have different origins, which are doping dependent and independent, respectively.

Due to the different resonance profiles in x'x' and x'y' geometry the drop of the phonon intensities can only be explained in the framework of a resonant theory which must account for the bands of the initial and final states. Calculations for the phonons of Y-123 in the superconducting state which have been performed by Heyen *et al.*[19] and which are based on the local-density approximation and the linear muffin-tin-orbital method do not show any signature of an intensity drop around 2 eV for xx/yy and zz symmetry. The calculated xx/yy intensity of the O(4) mode has a local intensity minimum at 2.0 eV but at 1.6 eV the predicted intensity is more than twice the intensity at 2.0 eV excitation energy which is strong contrast to our data.

As no appropriate theory is available we try an interpretation in a simple picture: The intensity drop is observed for the Cu(2) mode and, for excitation energies below $\hbar\omega_c$, for the plane-related O(2)-O(3) mode and for the x'x' O(4) mode. This indicates that plane bands are responsible for the observed resonance effect. In case of the O(4) mode two processes seem to contribute to the phonon intensity, as the strongly resonant x'x' intensity exhibits the drop below $\hbar\omega_c$ and the x'y' intensity shows no resonance and no superconductivity-induced effects. As the characteristic energy $\hbar\omega_c$ which separates the regions with and without the superconductivity-induced intensity drop is the same for the O(4) mode as for the O(2)-O(3) mode, we conclude that the relevant initial or final state bands are the same. Thus, we attribute the x'x' intensity to a process involving that plane bands. On the other hand the x'y' intensity is attributed to the chain bands. Another hint for this interpretation is that the pairing mechanism is believed to be located in the CuO_2 planes. Thus, superconductivity-induced effects would be expected for processes which involve plane bands.

Within a simple band structure picture the opening of the gap cannot explain the threshold of $\hbar\omega_c$ directly: If the opening of the gap would enhance the energy distance between the possible initial and final states for an allowed transition to a value which exceeds the excitation energy, this process would also be suppressed for lower excitation energies in the normal state. Figure 5 clearly shows that the behavior of the phonon intensity for 1.96 eV and 1.68 eV excitations is essentially the same. Thus, only a fundamental change of the band structure could explain the different behavior for blue and red excitation. As the x'x' intensity of the Cu(2) mode has its maximum right at the critical energy $\hbar\omega_c$ (see Fig. 6) the fundamental change with the superconducting transition should take place in a plane band involving the Cu(2) atom. As mentioned above the O(4) mode intensity in x'x' and x'y' symmetry results from different processes due to the coupling to the Cu(2)-O(2)-O(3) plane bands and to the Cu(1)-O(1) chain bands, respectively.

In comparison to the superconducting gap 2Δ the critical energy $\hbar\omega_c$ is quite a large energy. Superconductivity-induced high-energy effects have been observed previously by thermal difference reflectance (TDR) spectroscopy[14] and by ellipsometry.[13] In the ellipsometry data a crossing point in ε_2 at 2 eV separates two spectral regions of different behavior in their temperature dependencies. The TDR spectra of Y-123 and other high-temperature superconductors exhibit a deviation from unity in the ratio R_S/R_N of the superconducting to normal state spectra at high photon energies (≈2.0 eV). Within the Eliashberg theory the deviation can only be explained if the electron-boson coupling function contains a high-energy component in addition to the electron-phonon interaction leading to an order parameter which is non-zero for similar energies. The microscopic origin of the high-energy interaction is most likely a $d^9 - d^{10}\underline{L}$ Cu-O charge-transfer within the CuO_2 planes.[14]

The Cu(2) mode intensity seems to correlate with the charge-transfer excitation at about 2.1 eV. The intensity drop of this mode below T_c is independent of excitation energy and supports the interpretation of a modified charge-transfer-mechanism in the superconducting state. On the other hand the O(2)-O(3) mode in x'y' and the O(4) mode in x'x' geometry behave completely different for excitation energies above and below $\hbar\omega_c$. This indicates that the underlying mechanism is not the modified charge-transfer itself but the opening of the gap, which is non-zero for high energies as argued by Holcomb *et al.*[14] Thus, superconductivity-induced high-energy effects which cannot be detected in transport experiments, leave their signature in resonant Raman experiments through different behavior of the phonon intensity above and below $\hbar\omega_c$ as well as in other optical experiments.[13,14]

V. SUMMARY

A resonance enhancement of the integrated phonon intensity is observed for the O(4) mode in x'x' and for the O(2)-O(3) mode in x'y' polarization geometry. It results mainly from an intensity drop for temperatures below T_c at excitation energies less then $\hbar\omega_c \approx 2.1$ eV. This drop is also observed for the Cu(2) mode, which has its maximum x'x' intensity right at this excitation energy. We believe that the charge-transfer is responsible for the intensity drop of all three phonon modes, directly for Cu(2) and indirectly via the order parameter for O(4) and O(2)-O(3). As the x'y' intensity of the O(4) mode shows hardly any resonance we believe that its origin is completely different from the one of the x'x' intensity.

ACKNOWLEDGMENTS

The authors thank M. Rübhausen and M. V. Klein for stimulating discussions and for performing the ellipsometry measurements of Yb-123. Financial support of the Deutsche Forschungsgemeinschaft via the Graduiertenkolleg “Physik nanostrukturierter Festkörper” is gratefully acknowledged.

---

[*] Present Address: Basler AG, An der Strusbek 60-62, D-22926 Ahrensburg, Germany.

[1] E. Altendorf, X. K. Chen, J. C. Irwin, R. Liang, and W. N. Hardy, Phys. Rev. B **47**, 8140, 1993.

[2] V. G. Hadjiev, Xingjiang Zhou, T. Strohm, M. Cardona, Q. M. Lin, and C. W. Chu, Phys. Rev. B **58**, 1043, 1998.

[3] A. Bock, S. Ostertun, R. Das Sharma, M. Rübhausen, and K.-O. Subke, Phys. Rev. B **60**, 3532, 1999.

[4] R. Zeyher and G. Zwicknagel, Z. Phys. B **78**, 175, 1990.

[5] E. J. Nicol, C. Jiang, and J. P. Carbotte, Phys. Rev. B **47**, 8131, 1993.

[6] T. P. Devereaux, Phys. Rev. B **50**, 10287, 1994.

[7] B. Normand, H. Kohno, and H. Fukuyama, Phys. Rev. B **53**, 856, 1996.

[8] E. Ya. Sherman, R. Li, and R. Feile, Phys. Rev. B **52**, R15757, 1995.

[9] O. V. Misochko, E. Ya. Sherman, N. Umesaki, K. Sakai, and S. Nakashima, Phys. Rev. B **59**, 11495, 1999.

[10] T. Wolf, W. Goldacker, B. Obst, G. Roth, and R. Flukiger, J. Crystal Growth **96**, 1010, 1989.

[11] Y. Xu and W. Guan, Phys. Rev. B **45**, 3176, 1992.

[12] M. Rübhausen, C. T. Rieck, N. Dieckmann, K.-O. Subke, A. Bock, and U. Merkt, Phys. Rev. B **56**, 14797, 1997.

[13] M. Rübhausen, A. Gozar, M. V. Klein, P. Guptasarma, and D. G. Hinks, submitted to Phys. Rev. B

[14] M. J. Holcomb, C. L. Perry, J. P. Collman, and W. A. Little, Phys. Rev. B **52**, 6734, 1996.

[15] A. Bock, Ann. Phys. **8**, 441, 1999.

[16] J. L. Tallon, C. Bernhard, H. Shaked, R. L. Hitterman, and J. D. Jorgensen, Phys. Rev. B **51**, 12911, 1995.
[17] M. Rübhausen, O. A. Hammerstein, A. Bock, U. Merkt, C. T. Rieck, P. Guptasarma, D. G. Hinks, and M. V. Klein, Phys. Rev. Lett. **82**, 5349, 1999.
[18] B. Friedl, C. Thomsen, H.-U. Habermeier, and M. Cardona, Solid State Commun. **78**, 291, 1991.
[19] E. T. Heyen, S. N. Rashkeev, I. I. Mazin, O. K. Andersen, R. Liu, M. Cardona, and O. Jepsen, Phys. Rev. Lett. **65**, 3048, 1990.

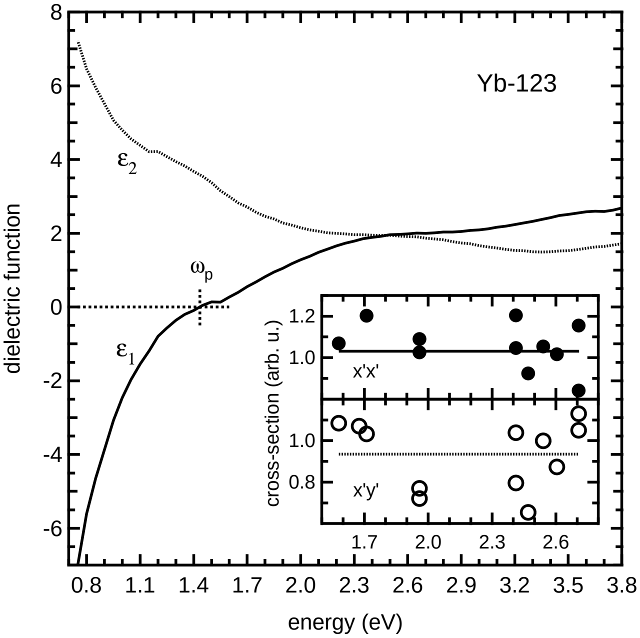

FIG. 1. Complex dielectric function $\varepsilon_1 + i\varepsilon_2$ of Yb-123 at room temperature. The inset depicts the Raman cross-section for the x'x' (top panel) and the x'y' (bottom panel) polarization symmetries. Lines mark the average values.

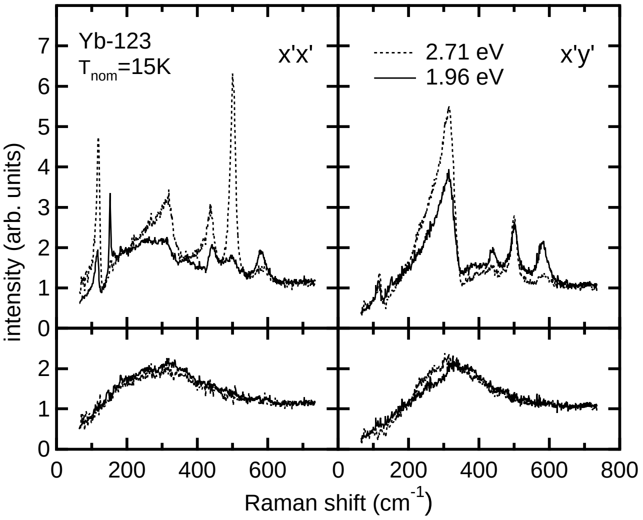

FIG. 2. Raman spectra of Yb-123 in x'x' and x'y' polarization geometries taken with excitation energies $\hbar\omega_i = 2.71$ eV (dashed lines) and 1.96 eV (solid) at 15 K cryostat temperature. The lower panels show the background spectra obtained by subtraction of the phonons.

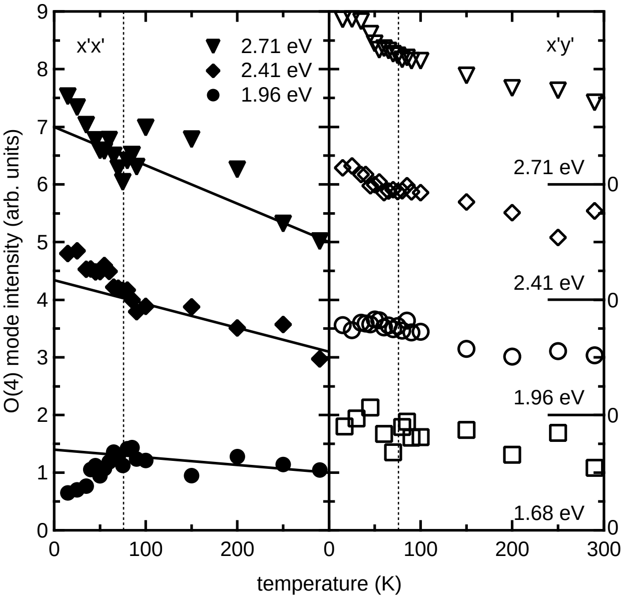

FIG. 3. Temperature dependence of the integrated O(4) Raman intensity in Yb-123 in x'x' (closed symbols) and x'y' (open symbols) polarizations for excitation energies 2.71 eV (triangles), 2.41 eV (diamonds), 1.96 eV (circles), and 1.68 eV (squares). Solid lines serve as guides to the eye, dashed lines indicate T_c. The x'y' data are offset as indicated.

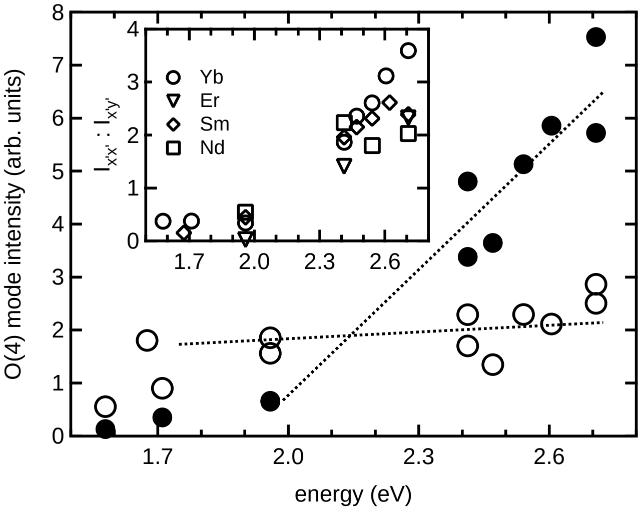

FIG. 4. O(4) intensity of Yb-123 at 15 K in x'x' (closed symbols) and x'y' (open symbols) polarization geometry. Lines are guides to the eye. The inset shows the ratio of the x'x' and x'y' intensity at 15 K for various R-123 single crystals that correspond to different doping levels.

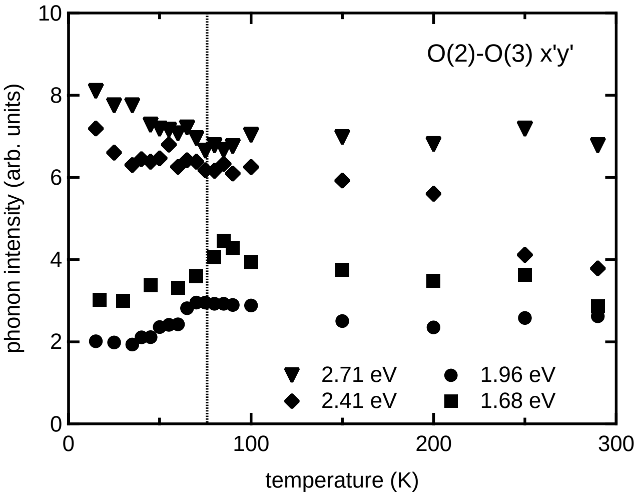

FIG. 5. Temperature dependence of the O(2)-O(3) intensity of Yb-123 for excitation energies $\hbar\omega_i = 2.71$ eV (triangles), 2.41 eV (diamonds), 1.96 eV (circles), and 1.68 eV (squares). The dotted line indicates T_c.

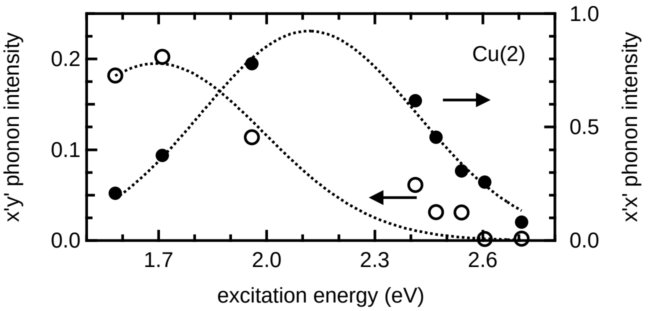

FIG. 6. Resonance of the intensity of the Cu(2) mode in Yb-123 at 15 K in x'x' (closed symbols) and x'y' (open symbols) geometry. Dotted Gaussian profiles guide the eye.